Fuel 284 (2021) 118880

Contents lists available at ScienceDirect

Fuel

journal homepage: www.elsevier.com/locate/fuel

Full Length Article

The influence of water-soluble inorganic matter on combustion of grape pomace and its chars produced by slow and fast pyrolysis

D.A. Mortari[a,*], D. Perondi[b], G.B. Rossi[a], J.L. Bonato[b], M. Godinho[b], F.M. Pereira[a]

[a] Mechanical Engineering Department, Federal University of Rio Grande do Sul, Porto Alegre, Rio Grande do Sul, Brazil
[b] Postgraduate Program in Engineering of Processes and Technologies, University of Caxias do Sul, Caxias do Sul, Rio Grande do Sul, Brazil

ARTICLE INFO

Keywords:
Water leaching
Biomass
Char combustion
Pyrolysis
NO formation
Ash
Drop tube furnace

ABSTRACT

The influence of water-soluble inorganic constituents on combustion of raw grape pomace (RGP) and its chars was investigated. Water leaching pretreatment was performed and the leached grape pomace (WLGP) and RGP samples were subsequently characterized by TGA to investigate the combustion under low heating rate. Then, the WLGP and RGP pyrolysis was carried out at slow (5 °C/min) and fast (120 °C/min) heating rates and the gas and char products were characterized. Finally, the combustion of RGP, WLGP, RGP chars and WLGP chars was analyzed in a drop tube furnace (DTF) to determine the influence of water-soluble inorganic matter on burnout and gas emissions. The water leaching pretreatment removed considerable amounts of K, B, Mg and P. The TGA results showed that the inorganic matter reduction negatively affected the combustion reaction rates, leading to a displacement to higher temperatures of ignition and burnout. Nevertheless, the DTF results showed no relevant effect on combustion efficiency between the RGP and WLGP samples. On the other hand, the pretreatment effect was pronounced during the WLGP chars combustion, in which the burnout of WLGP chars combustion was 30% lower compared to the RGP chars and 50% lower compared to the burnout obtained for raw samples. Additionally, the pretreatment affected the NO and CO formation, increasing the gas species concentrations during WLGP and WLGP chars' combustion.

1. Introduction

Many efforts have been devoted to enable the use of agroindustrial residues as a CO_2-neutral and renewable fuel for power generation [1,2]. A wide biomass variety is available for this purpose [3] and several effective technologies have been developed for its utilization, including combustion, pyrolysis, gasification and torrefaction [4,5]. However, there are many drawbacks of biomass application, such as the costs and transportation logistics between the feedstock generation site and the plant, the residues' physico-chemical characteristics and energy density, among others [6].

In this context, grape pomace is a byproduct with high potential for energy application since it is already generated in fruit processing plants, minimizing transportation costs. Grape is one of the most cultivated fruits in the world and the processing of fruit to produce juice, wine and other derivatives generates a considerable amount of residues [7]. World grape production is approximately 67 Mt per year and waste output amounts to 5 Mt [8]. The grape residues consist mainly of skins, seeds and stems, reaching up to 25% of the total weight [7,8]. A small percentage of the solid residue generated is used for secondary purposes such as production of wine alcohol, animal feed and compost fertilizer and extraction of grape seed oil and bioactive compounds [9], but the major part is disposed in open areas, and consequently causes environmental problems.

Concerning the physico-chemical characteristics of grape pomace and others agroindustrial residues, the biomass feedstock has high inorganic species content, with strong potential for damage to generation plant components, resulting in high maintenance costs besides the formation of acidic and toxic pollutants [10–12]. Water leaching can be used to upgrade biomass and can modify the fuel composition aiming at reducing the ash-related problems such as agglomeration, fouling, corrosion and slagging, generated in thermochemical conversion systems [10,13,14]. Previous studies have investigated the water leaching process for the removal of alkali and alkaline earth metals (AAEMs), sulfur and chlorine, finding it to be an effective and inexpensive process [10,13]. The modification of fuel by water leaching can improve the physico-chemical properties, affecting the ash content, ash fusibility, initial melting temperature and heating value [14]. The extracted leached liquid consists mainly of sugars and organic acids, and its recovery to produce alcohol and other coproducts is as feasible alternative to

* Corresponding author.
E-mail address: daniela.mortari@ufrgs.br (D.A. Mortari).

https://doi.org/10.1016/j.fuel.2020.118880
Received 24 May 2020; Received in revised form 30 July 2020; Accepted 2 August 2020
Available online 20 August 2020

reduce costs related to this pretreatment [10]. The water leaching procedure can even be performed by leaving biomass in the field after harvest, exposed to at least one rain episode [11]. However, controlled leaching is generally superior to natural leaching [15].

Experimental study using different biomasses, with distinct scales showed that water leaching pretreatment achieved about 90% chlorine reduction and 80% potassium reduction [16]. After the pretreatment, high temperature chlorine corrosion can be effectively reduced as well as the risk of alkali induced fouling [13]. Wang et al. (2018) [17] studied the water leaching pretreatment effect on ignition and formation of particulate matter with an aerodynamic diameter smaller than 1.0 μm ($PM_{1.0}$) during combustion of wheat straw. The results showed that the biomass functional groups were not affected by the pretreatment, but it increased the specific surface area (from 3.7 to 8.4 cm^2/g) and total pore volume (from 0.0063 to 0.0091 cm^3/g), in agreement with the results found by Zang et al. (2018) [18]. After water leaching, $PM_{1.0}$ emissions were reduced by 90%. The authors also reported ignition delay, but burnout occurred earlier [17]. This phenomenon can be explained by two hypotheses: 1- the increase in specific surface area and total pore volume led to greater gas diffusion inside the particles, improving the char combustion; or 2- after water leaching, the biomass particles had higher melting temperature, reducing the sintering effect, which decreased the particle's access to the active sites, and consequently enhanced char combustion [17]. In addition, the catalyst effect of water-soluble minerals is primarily observed in devolatilization. The TGA results showed that after pretreatment, devolatilization started at higher temperatures and ignition occurred at 17 °C above the temperature of the untreated sample [19]. These findings are consistent with previous studies reporting that alkali metals, particularly potassium, act as catalysts to promote release of volatiles [19,20]. There are also studies reporting pretreatment for inorganic removal followed by potassium doping, but most of these studies were performed using low heating rates [17]. Link et al. (2018) [15] investigated the leaching effect on the gasification products of wine and vine residues. The results showed higher CO and H_2 gas production for the leached residues during gasification, increasing the gas low heating value by 17%. The authors attributed this upgrade in gas product composition to the higher moisture content of the leached vine residue, favoring the carbon conversion. The pretreatment also lowered the tar yield and CH_4 and CO_2 formation [15]. Deng et al. (2019) [14] reported that after water leaching the ash fusion temperature increased significantly while the deposition mass decreased dramatically during biomass combustion. Zhang et al. (2018) [18] stated that inorganic species have significant effect on the torrefaction process of rice rusk. The removal of alkali and alkaline earth metals (AAEMs) affected the reaction routes, decreasing the solid product yield and increasing the gas product yield. The authors also observed a decrease of water content and increase of organic component content in the liquid products. Furthermore, recent research has reported that ash-forming species influence NO formation during biomass char combustion. During pyrolysis, part of the nitrogen content in fuel is released as volatiles (from 70 to 90% of the fuel-N) and part remains in the char matrix [4,21]. The ash-forming matter removal affects the conversion of char-N to NO and its reduction reactions [21,22]. The authors observed that the conversion of char-N to NO was almost 70% higher for the demineralized biomass compared to the raw samples.

Even though biomass-leaching pretreatments followed by torrefaction [23], carbonization [24] and combustion are discussed in the literature, to the best of our knowledge, there are no other studies dealing specifically with slow and fast pyrolysis of leached biomass followed by combustion of the resulting char under practicable heating rate conditions, as presented in this study. In this context, the understanding of ash-forming matter's influence on these thermal processes is of great importance to develop efficient technologies that can add value to alternative fuels.

In this study, the effect of water leaching pretreatment on grape pomace combustion and pyrolysis was investigated. The analysis focused on the combustion of chars produced via fast and slow pyrolysis in a DTF furnace, taking into account the ash-forming matter's effect on burnout and gas emissions. Additionally, pyrolysis yields were evaluated in terms of char, gas and liquid production. The samples were characterized before and after the water leaching, pyrolysis and combustion processes. TGA was also employed to investigate the water leaching effect during combustion and devolatilization, as well as to study the reaction kinetics.

2. Materials and methods

2.1. Biomass preparation and characterization

The agroindustrial residue used as a feedstock in this study was grape pomace (skin and seeds). The raw grape pomace (RGP) was provided by a local winery in Rio Grande do Sul State (South region of Brazil). The sample was dried for 24 h in an oven at 80 °C, then milled and sieved to reach particle size smaller than 2 mm.

To evaluate the ash-forming matter's effect on pyrolysis and combustion, half the sample was submitted to pretreatment where the raw grape pomace (RGP) was leached with distilled water at room temperature for 2 h. The dilution rate used was 1 g of sample per 20 mL of water (1:20). After bath with stirring, the water leached grape pomace (WLGP) sample was filtered and dried in an oven at 80 °C for 24 h. Finally, the entire amount of both samples (RGP and WLGP) was milled and sieved to attain average particle size of 75 μm for the thermogravimetric (TGA), pyrolysis and combustion experiments. The experimental development is shown in the diagram of Fig. 1.

The raw grape pomace (RGP) and the water-leached grape pomace

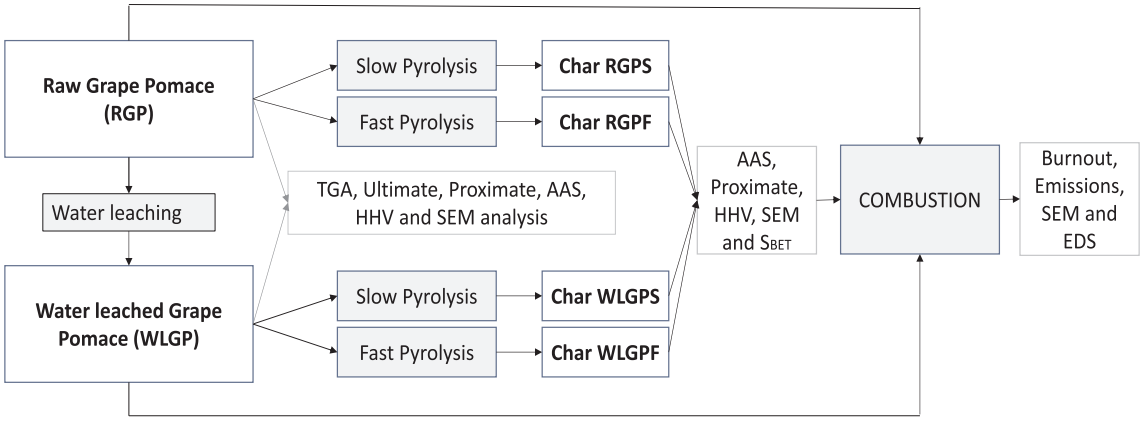

Fig. 1. Diagram of experimental development.

(WLGP) were characterized by thermogravimetric analysis (TGA), proximate analysis, ultimate analysis, higher heating value (HHV), main components (cellulose, hemicellulose, lignin and the extractives), scanning electron microscopy (SEM) and atomic absorption spectroscopy (AAS) to determine the contents of K, Ca, Mg, Cu, Zn, Fe, P, B, N, S and Mn. The proximate, ultimate and HHV analyses were performed according to the standards from the American Society for Testing and Materials (ASTM), based on D3172-89 (1993), D5373 (2008) and D5865-13 (2013), respectively. The main components analysis was performed according to the Van Soest gravimetric method [25].

2.2. Thermogravimetric experiments

The TGA experiments were performed with an STA 449 F3 Jupiter thermogravimetric balance (Netzsch). The thermal decomposition profiles of RGP and WLGP were evaluated under air and N_2 atmospheres to investigate combustion and devolatilization, respectively. For each experiment, the run temperature ranged from 25 °C to 700 °C and sample weight was 10 ± 0.5 mg. The heating rate applied in the combustion experiments was 10 °C/min and in the devolatilization experiments were 5, 10, 15 and 25 °C/min.

The diffusion limitation effects in the TG/DTG measurements were estimated according to the method proposed by Jess and Andresen, (2010) [26]. This method takes into account the temperature reached at 50% of char conversion, the content of the oxygen, the height of the crucible and the bulk density of the char sample. For operating conditions adopted in the TGA experiments, a maximum heating rate of around 300 °C/min was obtained, much higher than the highest heating rate (25 °C/min) used in the TGA experiments. Therefore, TGA experiments were performed in chemical control regime, without diffusion limitations (no intraparticle concentration gradient).

The ignition temperature was determined according to the method described in detail by Xiang-guo et al. (2006) [27], by applying TG and DTG curves. The method is based on identifying the intersection between specific reaction points during fuel thermal decomposition under air atmosphere. The method, definition of reaction points and results are shown in Fig. S1.

A kinetic study was performed to estimate the activation energy (E_α) related to the devolatilization process, in which the Friedman kinetic model was employed considering three heating rates – 5, 10 and 15 °C/min [28,29]. The E_α and standard deviations values were determined taking into account the conversion degrees in the range of 0.1 (10%)–0.9 (90%). The Friedman model consists of a differential isoconversional method (model-free method) that, for linear non-isothermal conditions (constant heating rates), is represented by Eq. [1]:

$$\ln\left(\beta\frac{d\alpha}{dt}\right)_{\alpha,i} = ln[f(\alpha)A_\alpha] - \frac{E_\alpha}{RT_{\alpha,i}} \quad (1)$$

where β is the heating rate, E_α is the activation energy, A_α is the pre-exponential factor and R is the universal gas constant. The model-free method consists of to determine activation energy E_α [kJ mol^{-1}] as a reaction conversion function (α). Thus, the activation energy is calculated from the slope of $\ln\left(\frac{d\alpha}{dt}\right)_{\alpha,i}$ against $\frac{1}{T_{\alpha,i}}$ at each α given [28]. The Eq. (1) is derived from Eq. (2) by applying the isoconversional principle.

$$\frac{d\alpha}{dt} = A\exp\left[\frac{-E}{RT}\right]f(\alpha) \quad (2)$$

This theory assumes that $\frac{d\alpha}{dt} = k(T)f(\alpha)$, where f(α) represents de reaction model and k(T) represents the Arrhenius reaction rate coefficient [30].

2.3. Fast and slow pyrolysis experimental setup

Fig. 2 shows the quartz fixed-bed reactor system used to investigate the fast and slow pyrolysis of RGP and WLGP. The reactor is electrically heated by two 1900 W resistors and has an internally portable quartz tube with dimensions of 981 mm in length, 49 mm in outer diameter and 41 mm in inner diameter. Two type-K thermocouples are positioned inside the reactor. The reactor exhaust outlet is connected to 10 bubblers used to retain the condensable gases and a flowmeter to measure the flow of gases produced during the pyrolysis process. Each bubbler was filled with 100 mL of isopropyl alcohol (except the first and the last) and kept in an ice bath at approximately −10 °C. Non-condensable gases were collected in SKC bags (FlexFoil PLUS Gas Sample Bags), after passing through the flowmeter for further chromatographic analysis.

The pyrolysis process of RGP and WLGP was conducted at high heating rate (120 °C/min) (denominated fast pyrolysis) and low heating rate (5 °C/min) (denominated slow pyrolysis). The N_2 flow inside the tube was 150 mL/min for all experiments. For the fast pyrolysis experiments, upon reaching 600 °C, 150 ± 0.5 g of biomass was quickly pushed into the fixed-bed reactor. The experiment remained in this condition for 30 min. For slow pyrolysis, the sample was fed into the quartz tube at room temperature and placed into the unheated reactor. The reactor temperature program was set to increase until 600 °C at 5 °C/min and remain at this temperature for 30 min. A particle holding time of 30 min was applied for both pyrolysis conditions in order to ensure that only the influence of the heating rate was being assessed. The non-condensable gases produced during the processes were continuously collected and stored in specific SKC bags.

The non-condensable gases (H_2, CO, CO_2 and CH_4), char and bio-oil generated from the pyrolysis process were quantified. The solid and gas fractions were also characterized. The non-condensable gases were characterized with a Gas Chromatograph (Dani Master GC). The detailed GC method is described by Perondi et al. (2017) [31]. The chars obtained under both pyrolysis conditions were weighed for yield calculation and characterized before the combustion experiments by proximate analysis, HHV, inorganic contents, SEM and specific surface area analysis (S_{BET}).

The specific surface area (S_{BET}) and pore size distribution were characterized by N_2 adsorption at 77 K in a Surface Area and Pore Size Analyzer (Quantachrome Instruments, Nova 1200, U.S.A). The samples (RGPS, RGPF, WLGPS and WLGPF) were outgassed under vacuum at 200 °C for 20 h prior to testing. The temperature used (200 °C) was selected to avoid the release of volatiles contained in the samples. The surface area was determined by the BET method and pore size distribution by the non-local density functional theory (NLDFT).

The chars produced by slow pyrolysis were denominated RGPS and WLGPS and the chars produced by fast pyrolysis were denominated RGPF and WLGPF.

2.4. Combustion experimental setup

The combustion of the RGP, WLGP and the chars produced during pyrolysis (RGPS, RGPF, WLGPS and WLGPF) was subsequently characterized in a drop tube furnace (DTF). The DTF used in this work was a cylindrical ceramic combustion chamber, electrically heated, with a useful length of 1232 mm and an inner diameter of 48 mm (Fig. 3a). The reactor chamber temperature control is built in three parts, each with three uniformly distributed type-K thermocouples: one for controlling and two for monitoring the wall furnace temperature. A water-cooled injector placed on the top of the reactor delivers solid fuel to the combustion chamber, carried by air. The samples are collected along the reactor by means of a water-cooled, nitrogen-quenched stainless-steel probe. After collection by the probe, the particle samples are retained by a quartz filter for subsequent analysis. The same stainless-steel probe is also used without nitrogen flow to measure the flue gas from combustion (NO, CO, SO_2, O_2 and CO_2). The flue gas was analyzed by a Siemens gas analyzer after being conditioned by filters and condenser.

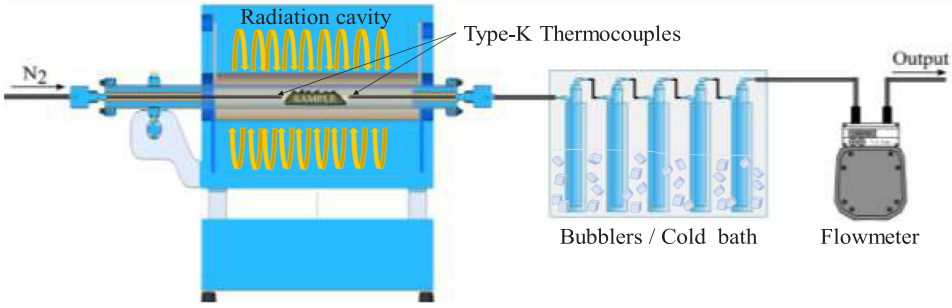

Fig. 2. The schematic of tubular fixed bed reactor system.

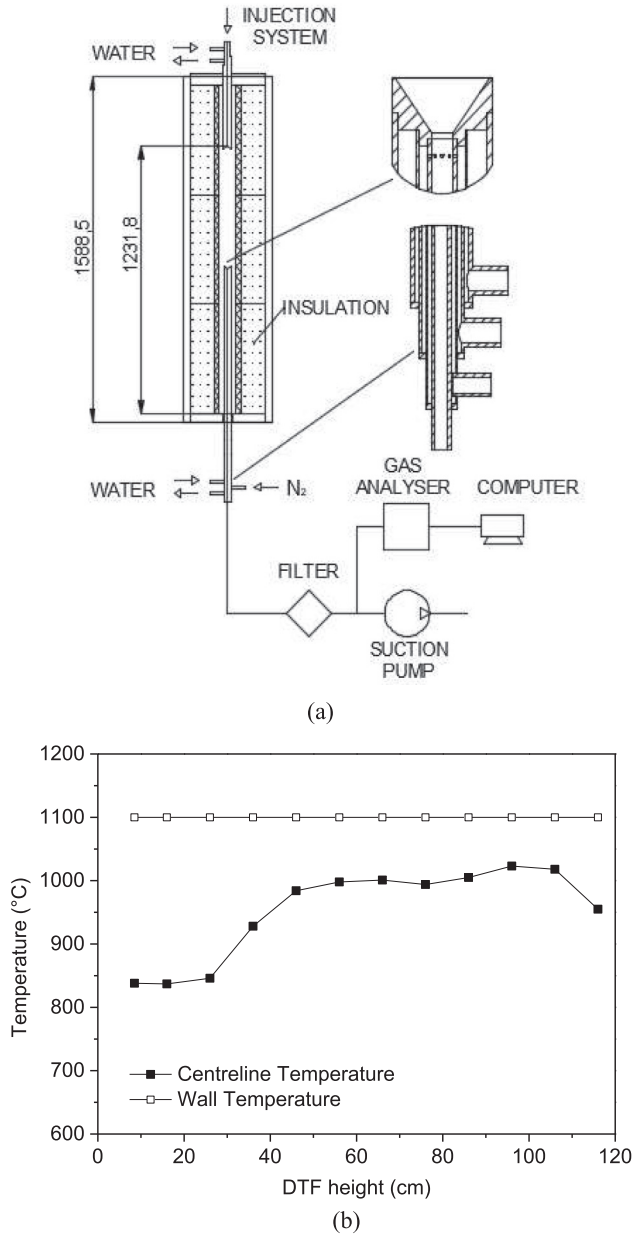

Fig. 3. (a) Schematic of drop tube system and (b) centerline temperature profile along the furnace.

The combustion experiments were performed at 1100 °C (wall temperature). A type-K thermocouple probe was used to obtain the temperature profile along the centerline of the reactor (Fig. 3b). The resulting residence time of the sample inside the furnace was approximately 280 ms (estimated by using the method proposed by Farrow et al., (2015) [32]. The sample mass flow rate applied was 32 g/h and the air flow rate was 30 L/min. The experiments to verify the repeatability of the DTF were performed with the RGP and WLGP samples.

The combustion yield was determined by means of the burnout (ψ), using the ash tracer method according to Eq. (3):

$$\psi = \left[1 - \left(\frac{\omega_f}{100 - \omega_f}\right) * \left(\frac{100 - \omega_x}{\omega_x}\right)\right] * 100 \quad (3)$$

where ω_f and ω_x are the mass fractions of ash (dry basis) in the original sample of biomass and in the collected residue from combustion, respectively.

3. Results

3.1. Samples characterization - water leaching results

The high heating value (HHV), proximate, ultimate and chemical composition analyses of RGP and WLGP are presented in Table 1. In addition, the proximate analysis and HHV results of chars obtained from pyrolysis are also presented. After water leaching, the content of moisture, volatile matter and extractives decreased. The most significant reduction was observed for the ash content (about 60%). On the other hand, the fixed carbon, cellulose, hemicellulose and lignin contents increased.

The inorganic element contents are presented in Table 2. The most relevant reductions were observed for K, B, Mg and P. The potassium content decreased significantly, similar to the results presented in the literature [14,19,33].

The SEM micrographs of RGP and WLGP are shown in Fig. 4. The

Table 1
Characterization of grape pomace samples.

Grape Pomace samples	RGP	WLGP	RGPS	RGPF	WLGPS	WLGPF
Proximate Analysis (wt%)						
Moisture	7.60	4.30	4.65	5.08	3.67	4.26
Volatile matter	72.9	67.3	24.6	36.5	24.6	17.7
Fixed carbon	14.9	26.5	61.9	51.0	70.3	76.4
Ash	4.67	1.87	13.5	12.5	5.08	5.91
Ultimate Analysis (wt%)						
Carbon	47.9	51.0	–	–	–	–
Hydrogen	6.5	6.9	–	–	–	–
Nitrogen	2.5	2.3	–	–	–	–
Oxygen*	38.0	37.9	–	–	–	–
Lignocellulose composition (wt%)						
Hemicellulose	9.2	14.2	–	–	–	–
Cellulose	5.7	7.5	–	–	–	–
Lignin	42.4	55.6	–	–	–	–
Extractives	16. 6	11.8	–	–	–	–
HHV (MJ/kg)	21.2	22.1	27.4	24.7	28.4	30.9

*By difference.

Table 2
Inorganic elements of grape pomace samples and chars produced from them.

Elements (g/kg)	RGP	WLGP	RGPS	WLGPS	RGPF	WLGPF
B	0.031	0.017	0.101	0.045	0.131	0.055
Ca	3.1	2.8	8.7	7.3	9.9	8.7
Cu	0.156	0.151	0.405	0.380	0.279	0.455
S	1.9	1.7	1.7	1.1	2.1	0.8
Fe	0.176	0.244	0.737	0.703	0.749	0.986
P	2.4	1.6	8.1	4.6	8.0	5.7
Mg	0.8	0.5	2.5	1.0	2.7	1.6
Mn	0.082	0.058	0.185	0.159	0.199	0.204
K	17.1	2.9	48.7	11.6	57.4	14.3
Zn	0.023	0.016	0.822	0.360	0.662	0.328
N	20.0	19.2	20.1	25.2	23.8	23.1

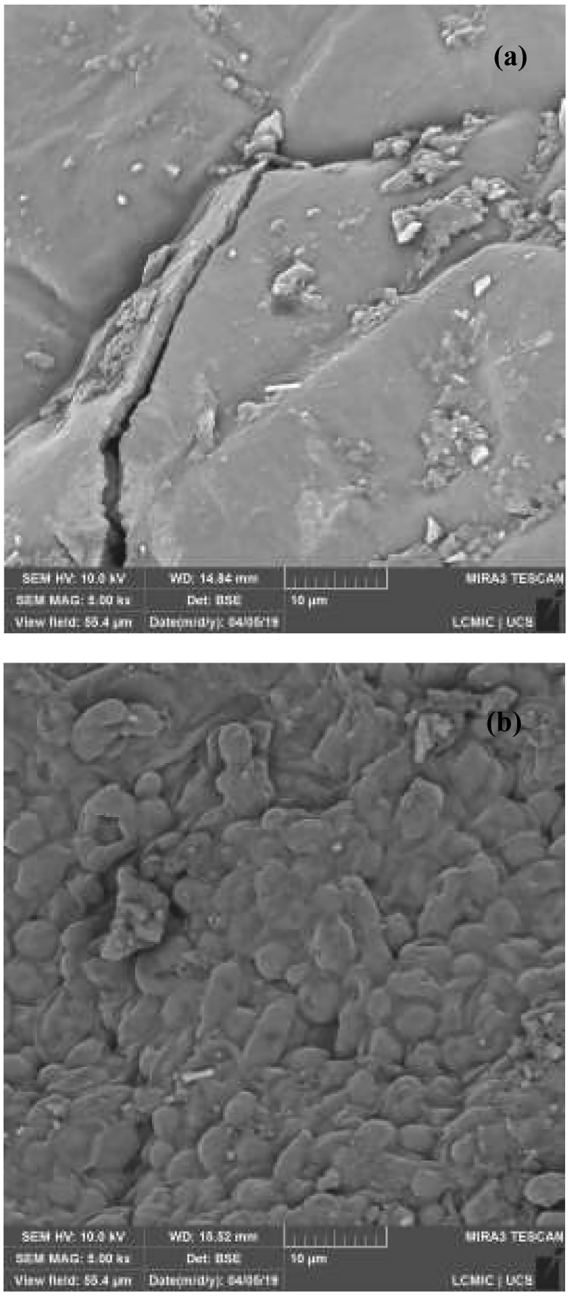

Fig. 4. SEM micrographs of (a) grape pomace (RGP) and (b) water leached grape pomace (WLGP) (magnification of 5000×).

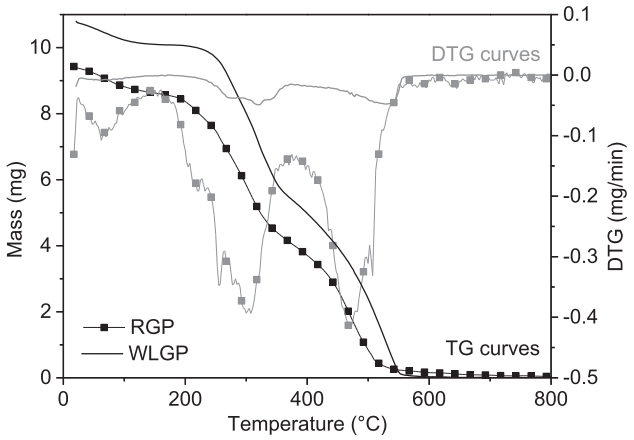

Fig. 5. TGA and DTG combustion curves obtained to the raw and water leached grape pomace under air atmosphere.

water leaching process modified the grape pomace structure, as can be observed in Fig. 4, showing a rougher surface, with interstitial regions resulting from the removal of mineral matter.

3.2. Thermogravimetric results

Fig. 5 shows the TG and DTG curves for RGP and WLGP under air atmosphere. According to the curves, the combustion process can be divided into three stages for both samples, related to the sample moisture evaporation (from room temperature to 110 °C), devolatilization (from 160 to 380 °C) and char oxidation (from 380 to 590 °C). These results are very close to those found in the literature [9]. The pretreatment displaced the combustion onset and the burnout to higher temperatures. While for RGP the combustion process started at 150 °C and the burnout was achieved at 553 °C, for WLGP the combustion started at 220 °C and the burnout took place at 565 °C. The most relevant difference between samples was the reaction rate, more notable in the DTG curves. While for raw RGP the reaction rate peaks reached of approximately 0.4 mg/s, for WLGP the highest decomposition peak reached 0.05 mg/s, indicating the strong effect of inorganic matter on combustion. Despite their thermally unstable characteristic, the biomass extractives also may have influenced the reaction rates during the combustion process at low temperatures (below 205 °C) [34]. The multiple sub-peaks observed for the devolatilization event in the DTG curves for both RGP and WLGP possibly can be attributed to the multistage occurrence and fluctuation of the organic matter combustion process, as reported by Sun et al. (2015) [35].

In addition, the ignition temperature evaluated by the method described by Xiang- guo et al. (2006) [27] showed that for the WLGP, the ignition temperature was 30 °C higher than that obtained for RGP (246 °C compared to 216 °C) (Fig. S1).

The results of TG and DTG curves obtained under N_2 atmosphere to evaluate devolatilization and its activation energy profile are presented in Fig. 6. According to the DTG curves (Fig. 6a and b), the mass loss was more intense between 150 °C and 400 °C due to the release of volatile matter, which consists of CO, CO_2 and condensable tar compounds from hemicelluloses and cellulose chain decomposition [36]. The DTG peaks related to the devolatilization reaction rates became more evident as the heating rate increased. For this reason, the water leaching effect on devolatilization was greater in the curve obtained at 25 °C/min. Evaluating the effect of the pretreatment, the devolatilization started at approximately 150 °C for RGP and at 170 °C for WLGP. The displacement to higher temperatures may be attributed to the extractive reduction, as presented in Table 1. In addition, the RGP DTG curves presented a double peak according to which both achieved maximum reaction rate of 1.0 mg/min, while for the WLGP the first peak (between

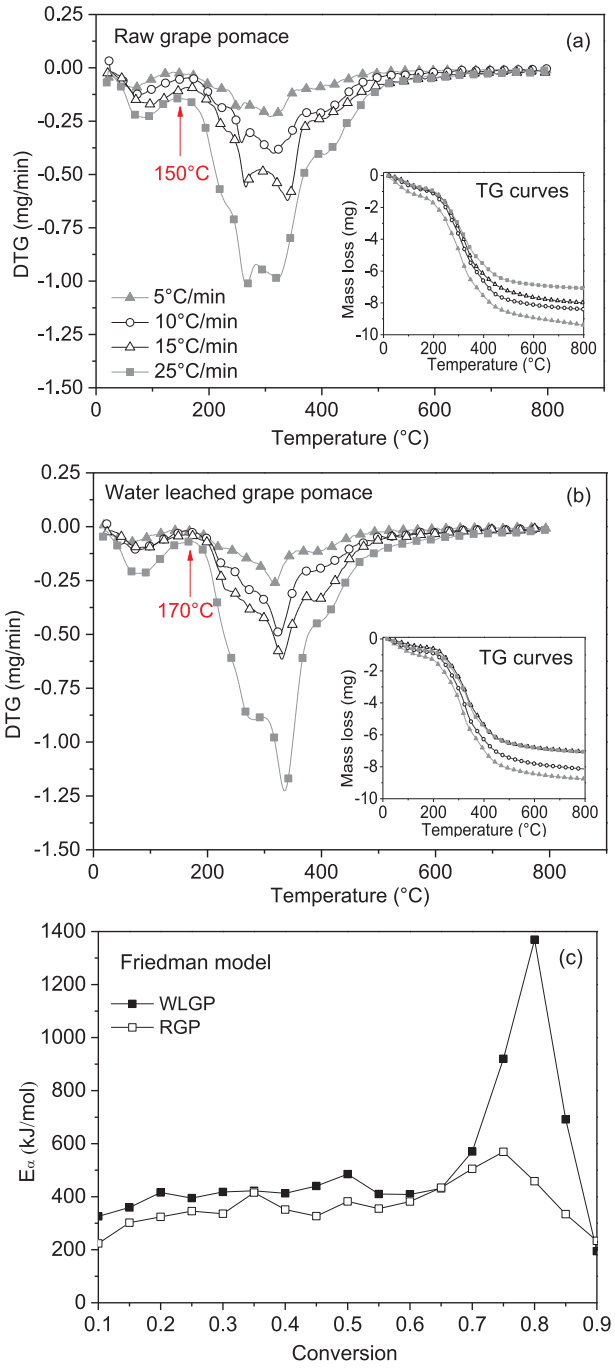

Fig. 6. TG/DTG curves of (a) RGP and (b) WLGP under N_2 atmosphere at 5, 10, 15 and 25 °C/min. (c) Activation energy (E_α) versus conversion (α) profiles of RPG and WLPG samples thermal decomposition.

200 and 300 °C) indicated a reaction rate of 0.85 mg/min and the second peak (between 300 and 400 °C) a maximum rate 1.25 mg/min.

The activation energy values (E_α) obtained by Friedman model for the WLPG were greater than for the RGP over the entire conversion range, indicating its lower reactivity. While the initial E_α value for RGP was approximately 200 kJ/mol, for WLGP the initial E_α value was approximately 300°kJ/mol. The higher activation energy obtained for WLGP at the beginning of the reaction can be associated with its lower extractives content in sample [34]. The variations in E_α peaks (Fig. 6c) indicate changes in reaction mechanisms, reinforcing the hypothesis of multistep reaction presented in the DTG curves of Figs. 5, 6a and 6b [36]. In addition, after the plateau from α = 0.1 to 0.7, there was a high increase in apparent activation energy for both samples. In the literature, the greater energy barrier after 70% of conversion can be attributed to the highly endothermic charring reactions during the pyrolysis experiments [36]. However, the aforementioned energy barrier was greater for WLGP. The WLGP thermal decomposition presented peaks exceeding 1300 kJ/mol, indicating the slow kinetics of charring reactions due to the absence of mineral matter catalytic effect. Considering the temperature average of the three heating rates applied, 70% of conversion was achieved at approximately 370 °C for RGP and 380 °C for WLGP.

Previous studies have indicated that AAEMs, especially potassium, act as catalysts for the crosslinking reactions of volatiles [19,37]. The ash-forming species may enhance the decomposition of volatile macromolecules, cracking the tar during pyrolysis and increasing the devolatilization yield. The samples' reactivity is also affected. Consequently, the TGA results of WLGP showed lower reaction rates during combustion and devolatilization, while a shift to higher temperatures in the devolatilization step and burnout was observed. In addition, the ignition temperature was 30 °C higher for WLGP samples. The thermal decomposition events that occur at low temperature, such as the devolatilization start and ignition, may also be influenced by the slight reduction in biomass extractives after the water leaching pretreatment. The activation energy profiles presented higher peaks after 65% conversion, suggesting a shift in reaction mechanism compared to the RGP sample and the existence of a higher energy barrier, corroborating previous studies reporting the catalytic effect of alkaline metals [19].

3.3. Pyrolysis experiments

The pyrolysis of RGP and WLGP was performed using slow and fast heating rates. In this study, the focus was on char investigation, but the gas and bio-oil products were also quantified. Fig. 7 shows the impact of water leaching pretreatment and heating rate on the distribution of pyrolysis products. Fig. 7a shows the product yields obtained from slow (RGPS and WLGPS) and fast (RGPF and WLGPF) pyrolysis processes. Fig. 7b shows the characterization of gas products (N_2 free basis).

As can be seen in Fig. 7a, the bio-oil yield (oil + condensed water) increased from 41.4% to 43.9% for the RGP samples and, from 39.4% to 43.9% for the WLGP samples as the heating rate increased from 5 to 120 °C/min. Demiral and Ayan (2011) [38] observed the same trend and attributed the higher yield of liquid products to the reduction of the heat and mass transfer limitations under higher heating rates. The high heating rate creates steep gradients within the particle, increasing the heat and mass transfer with the surroundings. Regarding the pretreatment effect, when the pyrolysis heating rate was shifted from slow to fast, the increase in bio-oil production was more pronounced for WLGP samples, associated with the mineral matter reduction. The lower inorganic content can suppress the magnitude of vapor cracking, leading to a reduction of gas and water formation, hence, increasing the bio-oil yield [20].

The gas yield was very similar for all processes (22.1 ± 1.2%), except for RGPF (12.8%). However, the gas composition changed significantly. The RGPS generated the highest H_2 concentration (30.9%) while WLGPF generated the lowest (7.0%). In general, the pretreatment led to lower H_2 and higher CO and CH_4 formation. The H_2 formation can be attributed to the cracking and deformation of the C=C and C–H bonds of the aromatic rings present in the biomass structure, as well as the cyclization and cracking processes of the primary pyrolytic vapors [39]. When the residence time of gases is reduced, there is also a tendency for reduction of H_2 formation. For this reason, the concentrations of H_2 obtained in fast pyrolysis were lower. The gas HHVs were higher for the WLGPS and WLGPF samples – 7.53 and 3.84 MJ/Nm^3, especially due to the higher CH_4 concentration, while for the RGPF and RGPS samples the HHVs were 2.54 and 2.78 MJ/Nm^3, respectively.

Regarding the char formation, it is well established in the literature that char yields decrease as the heating rate and temperature increase

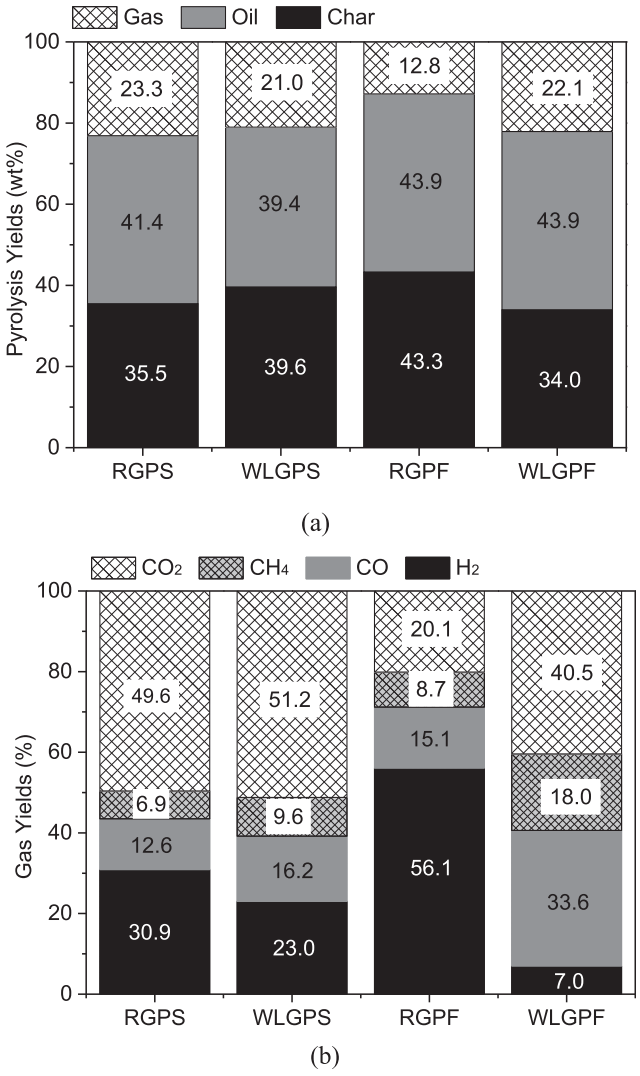

Fig. 7. (a) Products distribution and (b) Gas products (N_2 free basis) from slow and fast pyrolysis of raw grape pomace (RGP) and water leached grape pomace (WLGP).

[20,38]. Although the major product of fast pyrolysis is the bio-oil, the char produced from this condition is also a product of the reaction; hence, it is important to address an application for this product. The biomass char has properties closer to coal than raw biomass, allowing their use in existing plants with the minimum of necessary modifications. In our experiments, the char yield decreased from 39.6% to 34.0% for WLGP whereas it increased from 35.5% to 43.3% for RGP as the heating rate increased from 5 to 120 °C/min. The increase in char yield for RGP was unexpected, but may be associated with the formation of secondary char. Low heating rates and long residence times of volatiles in the particle lead to the predominance of secondary reactions (cracking, reforming, dehydration, condensation and polymerization), with tar cracking to form lighter compounds and char. On the other hand, during high heating rates, a low molecular weight metaplast is formed due to the fast bond breaking, leading to an increased pressure inside the particle, fast volatiles evaporation and low char yield [40]. At high heating rate, an increase in char yield was observed, as well as a reduction in gas yield. However, further studies should be performed to clarify the mechanisms involved during these processes.

With respect to the pretreatment effect, under fast pyrolysis the char yield of WLGP decreased. The mineral matter promotes the charring reaction and the formation of secondary char [20]. Thus, the reduction of inorganics in the biomass caused by the water leaching negatively affected the char formation. On the other hand, this effect was not observed under slow pyrolysis. A possible explanation is that with slow heating rate, the reduction of inorganic elements can increase the thermal stability of the samples, resulting in higher char formation [20].

The physico-chemical characteristics of the formed char changed drastically as the pyrolysis conditions shifted from slow to fast and from RGP to WLGP. Table 1 shows the proximate analysis and HHV and reveals that the pyrolysis processes increased the HHV, fixed carbon and ash content, while volatile matter content decreased. The most relevant fixed carbon concentration was obtained for the WLGPS and WLGPF samples. The devolatilization during slow pyrolysis was higher for RGP than WLGP considering that the final percentage was the same for both samples. However, the devolatilization during fast pyrolysis was approximately two times that of the WLGP sample.

The inorganic elements are presented in Table 2. The water leaching pretreatment removed a significant amount of water-soluble inorganic constituents, mainly potassium. The pyrolysis process removed part of the organic matter and led to notable increases of B, Ca, Cu, Fe, P, Mn, K and Zn concentrations.

Regarding the samples' structure, Fig. S2 shows the SEM images of formed chars from slow and fast pyrolysis and Fig. S3 shows the results of pore size distribution and specific surface area of chars. The pore size distribution data reveal that the pores of the chars obtained from grape pomace (RGPS, RGPF, WLGPS and WLGPF) were mostly mesoporous. It was also possible to verify a narrower pore region in the pyrolyzed materials with slow heating rate (both for WLGPS and for RGPS). This result can be explained by the following hypothesis, suggested by Della Rocca et al. (1999) [41]. For slow heating rates, volatile pyrolysis products are released through the natural porosity and no major change takes place in the particle morphology. On the other hand, for fast heating rates, the original cell structure is lost [42] because of melting phenomena [43–45]. Fast release of volatiles produces substantial internal overpressure and coalescence of the smaller pores, leading to large internal cavities and a more open structure of both wood [46] and lignin [43].

3.4. Combustion experiments

The reactivity of formed char and raw samples was investigated by means of DTF combustion experiments. The burnout results are presented in Fig. 8. The DTF experiments repeatability is evidenced by the low standard deviation obtained for the replicates performed with the WLGP and RGP samples (0.48% and 0.51%, respectively).

The differences in reactivity between raw samples (RGP and WLGP) and the chars (RGPS, RGPF, WLGPS and WLGPF) are clear. The highest

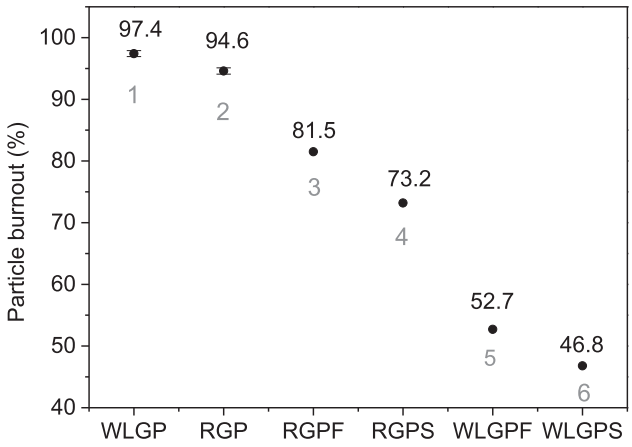

Fig. 8. Burnouts obtained from combustion of all fuel samples at 280 ms of residence time.

burnouts were obtained for RGP and WLGP (94.2 and 97.7%, respectively) due to their higher content of volatile matter and lower content of fixed carbon. The slight difference between the two samples (conditions (1) and (2) in Fig. 8) can possibly be attributed to the changes in surface and ash removal caused by the water leaching pretreatment (Fig. 4). Additionally, the catalytic effect of minerals was not evidenced in the combustion of raw samples. On the other hand, the catalytic effect becomes evident when the burnouts of WLGP char samples are compared to RGP chars under both pyrolysis conditions. The burnouts were approximately 30% lower for the WLGP chars combustion. In addition, when the combustion of WLGP char is compared to the combustion of WLGP, the difference is near 50% lower.

Evaluation of the char combustion as a function of pyrolysis conditions showed that the burnout was higher for the chars formed under fast pyrolysis for both RGP and WLGP. The increase of the char reactivity with the higher heating rate during pyrolysis can be explained by the occurrence of gasification reactions mainly on the surface of large pores, and/or a higher concentration of active sites [43]. Overall, it is expected that the higher the volatile matter content and lower fixed carbon, the higher the burnout will be. However, this trend was not observed during the combustion of WLGP chars, in which the WLGPF char formed under fast pyrolysis presented lower volatile matter content (Table 1) than the WLGPS char formed under slow pyrolysis (points 5 and 6 of Fig. 8). In addition, the burnout results were directly related to the S_{BET} results, as can be identified in Fig. S3c. The highest burnout values were obtained for chars with greater surface area. According to [47], oxidation rates are expected to be higher for chars with higher surface areas. Evaluation of char combustion as a function of pretreatment indicated the burnout was higher for RGP chars and these chars also presented higher S_{BET}.

The SEM images of the particle structures evaluated after DTF experiments, related to each burnout result (highlighted by the numbers in Fig. 8) are presented in Fig. 9, following a decreasing order of burning efficiency. According to Fig. 9, the higher the burnout, the greater was the apparent porosity of the residue. It is clear that during combustion the active sites of natural samples were completely accessed, resulting in very porous structures, poor in carbon (supported by the Supplementary material presented in Figs. S4 and S5). On the other hand, as the burnout decreased, the particle structure became less accessible, with a preserved structure, still containing high carbon content, which could have been converted with application of longer residence. In general, the pretreatment followed by pyrolysis produced a more thermally stable solid fuel.

The NO, CO, SO_2 and CO_2 concentrations obtained during combustion of RGP, WLGP and their chars produced under slow and fast pyrolysis are presented in Fig. 10. All emissions were measured at the same residence time, corresponding to the burnouts of Fig. 8. For comparison, the emissions were corrected to 10% of O_2 and were normalized by the maximum value. The high CO emission reflects the incomplete combustion due to the short residence time applied (280 ms) for the purpose of comparison, since longer residence times would cause complete combustion.

The NO emissions were higher for the WLGP samples, even with the lowest burnouts among the samples. Additionally, the nitrogen content of the WLGP samples was lower than the RGP samples. This result can be attributed to the influence of water leaching on NO formation. Karlström et al. (2017) [21] investigated the role of ash-forming elements on the NO formation during char combustion and verified that the conversion of char-N to NO was higher for the leached biomass compared to the raw samples. The catalytic effect of ash enhances the reduction of the initially formed NO to N_2 according to the global reaction ($NO + C \rightarrow {}^1/_2N_2 + CO$) [21,48]. The two reaction mechanisms proposed by the authors involving the influence of the catalytically active ash-forming element (M) suggest that the reduced catalytic sites ($\text{-}M_xO_y$) together with a carbon site (-C) dissociate NO, resulting in an oxidized catalytic site ($\text{-}M_xO_{y+1}$) and an active carbon site linked to nitrogen (-CN). Then the oxidized catalytic site ($\text{-}M_xO_{y+1}$) is regenerated by reacting with a carbon site [21,22]. Furthermore, the conversion of char-N to NO was investigated as a function of nitrogen content and the NO formation decreased as the nitrogen content in samples increased [22]. These results imply that both parameters influence the conversion of char-N to NO, and the several reactions proposed to explain the NO conversion mechanisms can occur simultaneously or compete [21,22]. In addition, the presence of CO has been reported to enhance the reduction of NO [21,22,48]. In this study, the combustion of WLGP chars produced more CO than the RGP chars. However, further research is required to confirm the relation between NO and CO formation.

The SO_2 emissions were more affected by the pyrolysis conditions than the water leaching pretreatment. Although similar studies using coal have reported that the soluble minerals in samples may reduce the SO_2 emissions during combustion [49], the highest SO_2 produced during the raw WLGP combustion can be attributed to the highest char conversion.

In general, the use of biomass via direct combustion and co-combustion for energy production still faces challenges due to ash-related issues, transportation expenses and grindability problems [11,13,50]. The inorganic elements present in biomass are limiting factors to its utilization due to the high potential for damage to generation plant components due to sintering and fouling, which reduce boiler efficiency and increase maintenance costs [12,37]. In this respect, the water leaching pretreatments improved the biomass and minimized these shortcomings. On the other hand, there are many studies concerning the catalytic effect of ash forming elements on combustion reactions.

Based on our findings, the water-soluble inorganic matter was successfully reduced by the water leaching and the biomass reactivity was clearly affected by this pretreatment. Nevertheless, while the TGA results showed reduction in combustion reaction rates, increased burnout and ignition temperatures and higher activation energy for the WLGP sample, the DTF results showed no relevant effect on combustion efficiency between the RGP and WLGP samples. However, the pretreatment effect cannot be neglected during the WLGP chars combustion, in which the burnout of WLGP chars was 50% lower than the burnout of RGP and WLGP samples and, 30% lower than the RGP chars. These findings for WLGP chars' combustion indicated that more attention is required to adjust the operational conditions. The advantage of less severe ash-related problems for boiler maintenance and efficiency is achieved at the expense of reduced char reactivity, which has to be dealt with during combustion control. The residues obtained after combustion showed a structure rich in carbon, suggesting that longer residence times are required for the WLGP char combustion. Moreover, more efforts should be dedicated to investigate the advantages related to biomass ash reduction regarding energy balance, considering extending power plants' life cycle.

4. Conclusions

This study investigated the effect of water leaching on combustion of grape pomace and its chars produced under slow and fast pyrolysis. The water leaching pretreatment improved the fuel characteristics in terms of reduction of ash and inorganic matter, mainly K. However, due to the catalytic effect of mineral matter, after the pretreatment the TGA results showed reduction in combustion reaction rates and increases of the ignition, devolatilization and burnout temperatures.

During pyrolysis, the water leaching pretreatment led to a higher bio-oil yield due to the suppression of cracking vapor reactions caused by the inorganic matter reduction. In addition, the gas products showed higher concentrations of CO and CH_4 and lower H_2. The gas HHV was higher for the WLGP samples. Regarding char formation, under fast pyrolysis the pretreatment led to a lower char yield. Moreover, the volatile matter and ash decreased while fixed carbon increased, so the pretreatment increased the char HHV.

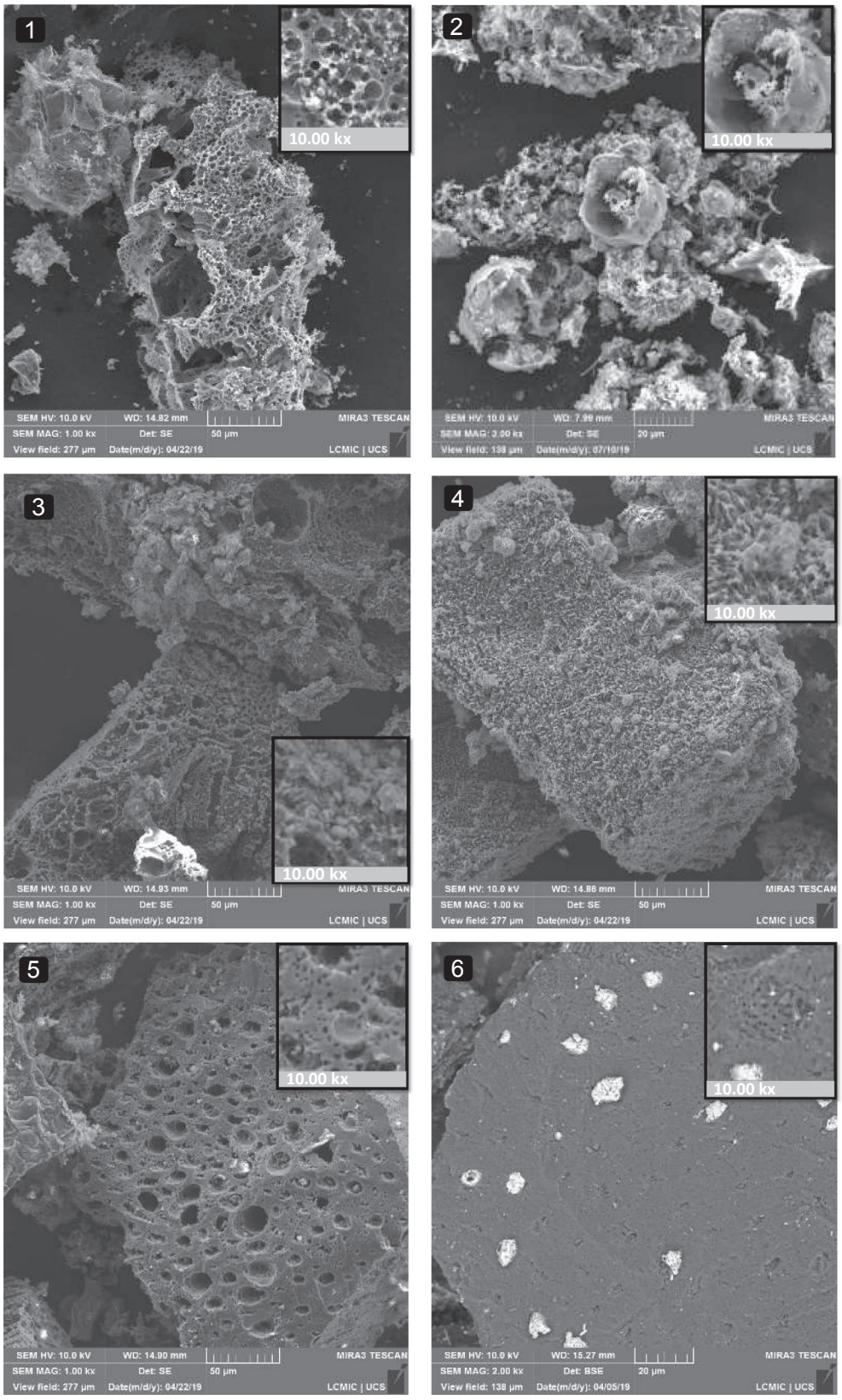

Fig. 9. SEM micrographs of DTF residues obtained after the combustion process, following a decreasing order of burning efficiency as in Fig. 8.

Finally, even though no relevant difference was observed in the burnout in the DTF of raw samples (WLGP and RGP), the burnout temperatures of the WLGP chars were 30% lower than RGP chars and 50% lower than raw samples. Additionally, the water-soluble inorganic reduction had a negative influence on the gas species formation, increasing the NO and CO emissions during WLGP and WLGP chars' combustion.

From a combustion application point of view, water leaching proved

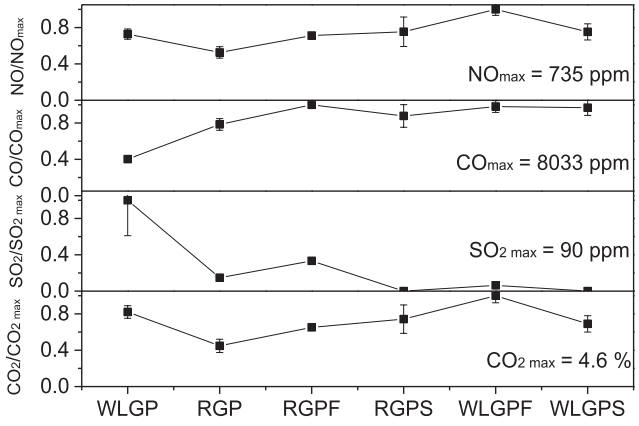

Fig. 10. Gas species concentration obtained at 280 ms of residence time, corrected to 10% of O_2.

to be effective in reducing the inorganic matter content, which tends to reduce problems related to ash deposition and corrosion in boilers. It also improved the HHV of the syngas and char produced by pyrolysis. On the other hand, the water leaching tended to reduce the reactivity of the pyrolytic chars, which may require longer residence times in the boiler to achieve complete burnout.

CRediT authorship contribution statement

D.A. Mortari: Conceptualization, Methodology, Validation, Investigation, Writing - review & editing. **D. Perondi:** Conceptualization, Methodology, Validation, Writing - review & editing, Visualization. **G.B. Rossi:** Methodology, Visualization. **J.L. Bonato:** Methodology, Visualization. **M. Godinho:** Supervision, Visualization, Writing - review & editing, Resources. **F.M. Pereira:** Supervision, Visualization, Resources, Writing - review & editing, Funding acquisition.

Declaration of Competing Interest

The authors declare that they have no known competing financial interests or personal relationships that could have appeared to influence the work reported in this paper.

Acknowledgments

We acknowledge the Office to Improve University Personnel of the Brazilian Ministry of Education (CAPES) for financial support (grant 88882.316272/2019-01) and, the National Council for Scientific and Technological Development (CNPq) (grant 310274/2018-4).

Appendix A. Supplementary data

Supplementary data to this article can be found online at https://doi.org/10.1016/j.fuel.2020.118880.

References

[1] McKendry P. Energy production from biomass (part 1): overview of biomass. Bioresour Technol 2002;83:37–46.
[2] Mao G, Huang N, Chen L, Wang H. Research on biomass energy and environment from the past to the future: A bibliometric analysis. Sci Total Environ 2018;635:1081–90.
[3] Saidur R, Abdelaziz EA, Demirbas A, Hossain MS, Mekhilef S. A review on biomass as a fuel for boilers. Renew Sustain Energy Rev 2011;15:2262–89.
[4] Liu X, Luo Z, Yu C. Conversion of char-N into NO_x and N_2O during combustion of biomass char. Fuel 2019;242:389–97.
[5] Hameed S, Sharma A, Pareek V, Wu H, Yu Y. A review on biomass pyrolysis models: Kinetic, network and mechanistic models. Biomass Bioenergy 2019;123:104–22.
[6] Bajwa DS, Peterson T, Sharma N, Shojaeiarani J, Bajwa SG. A review of densified solid biomass for energy production. Renew Sustain Energy Rev 2018;96:296–305.
[7] Ping L, Pizzi A, Guo ZD, Brosse N. Condensed tannins from grape pomace: Characterization by FTIR and MALDI TOF and production of environment friendly wood adhesive. Ind Crops Prod 2012;40:13–20.
[8] Mäkelä M, Kwong CW, Broström M, Yoshikawa K. Hydrothermal treatment of grape marc for solid fuel applications. Energy Convers Manage 2017;145:371–7.
[9] Botelho T, Costa M, Wilk M, Magdziarz A. Evaluation of the combustion characteristics of raw and torrefied grape pomace in a thermogravimetric analyzer and in a drop tube furnace. Fuel 2018;212:95–100.
[10] Yu C, Thy P, Wang L, Anderson SN, VanderGheynst JS, Upadhyaya SK, et al. Influence of leaching pretreatment on fuel properties of biomass. Fuel Process Technol 2014;128:43–53.
[11] Niu Y, Lv Y, Zhang X, Wang D, Li P, Hui S. Effects of water leaching (simulated rainfall) and additives (KOH, KCl, and SiO_2) on the ash fusion characteristics of corn straw. Appl Therm Eng 2019;154:485–92.
[12] Deng L, Zhang T, Che D. Effect of water washing on fuel properties, pyrolysis and combustion characteristics, and ash fusibility of biomass. Fuel Process Technol 2013;106:712–20.
[13] Abelha P, Vilela CM, Nanou P, Carbo M, Janssen A, Leiser S. Combustion improvements of upgraded biomass by washing and torrefaction. Fuel 2019;253:1018–33.
[14] Deng L, Jin X, Long J, Che D. Ash deposition behaviors during combustion of raw and water washed biomass fuels. J Energy Inst 2019;92:959–70.
[15] Link S, Arvelakis S, Paist A, Liliedahl T, Rosén C. Effect of leaching pretreatment on the gasification of wine and vine (residue) biomass. Renewable Energy 2018;115:1–5.
[16] Wang W, Bai S, Jin Q, Li S, Li Y, Li Y, et al. Soot formation during biomass pyrolysis: Effects of temperature, water leaching, and gas-phase residence time. J Anal Appl Pyrol 2018;134:484–94.
[17] Wang X, Adeosun A, Hu Z, Xiao Z, Khatri D, Li T, Tan H, Axelbaum RL. Effect of feedstock water leaching on ignition and $PM_{1.0}$ emission during biomass combustion in a flat-flame burner reactor. Proc Combust Inst 2018:1–9.
[18] Zhang S, Su Y, Ding K, Zhu S, Zhang H, Liu X, et al. Effect of inorganic species on torrefaction process and product properties of rice husk. Bioresour Technol 2018;265:450–5.
[19] Wang M, Liang F, Tian J, Chang L. Effects of mineral matters on the interactions between lignite and corncob during temperature-programmed co-pyrolysis. J Therm Anal Calorim 2019;138:1477–86.
[20] Persson H, Yang W. Catalytic pyrolysis of demineralized lignocellulosic biomass. Fuel 2019;252:200–9.
[21] Karlström O, Perander M, DeMartini N, Brink A, Hupa M. Role of ash on the NO formation during char oxidation of biomass. Fuel 2017;190:274–80.
[22] Ulusoy B, Lin W, Karlström O, Li S, Song W, Glarborg P, et al. Formation of NO and N_2O during raw and demineralized biomass char combustion. Energy Fuels 2019;33:5304–15.
[23] Vamvuka D, Loukakou E, Sfakiotakis S, Petrakis E. The impact of a combined pretreatment on the combustion performance of various biomass wastes and their blends with lignite. Thermochim Acta 2020;688:178599.
[24] Wang W, Wen C, Liu T, Li C, Xu J, Liu E, et al. Emission reduction of PM_{10} via pretreatment combining water washing and carbonisation during rice straw combustion: Focus on the effects of pretreatment and combustion conditions. Fuel Process Technol 2020;205:106412.
[25] Van Soest PJ, Wine RH. Development of lignin and cellulose in acid detergent fiber with permanganate. J Assoc Off Anal Chem 1968;51:780–5.
[26] Jess A, Andresen AK. Influence of mass transfer on thermogravimetric analysis of combustion and gasification reactivity of coke. Fuel 2010;89:1541–8.
[27] Xiang-guo L, Bao-guo M, Li X, Zhen-wu H, Xin-gang W. Thermogravimetric analysis of the co-combustion of the blends with high ash coal and waste tyres. Thermochim Acta 2006;441:79–83.
[28] Vyazovkin S, Burnham AK, Criado JM, Pérez-Maqueda LA, Popescu C, Sbirrazzuoli N. ICTAC Kinetics Committee recommendations for performing kinetic computations on thermal analysis data. Thermochim Acta 2011;520:1–19.
[29] Vyazovkin S, Chrissafis K, Di Lorenzo ML, Koga N, Pijolat M, Roduit B, et al. ICTAC Kinetics Committee recommendations for collecting experimental thermal analysis data for kinetic computation. Thermochim Acta 2014;590:1–23.
[30] Mortari DA, Britto MC, Crnkovic PM. Correlation between activation energy and thermal decomposition yield of sugarcane bagasse under CO_2/O_2 and N_2/O_2. Chem Eng Trans 2014;37:31–6.
[31] Perondi D, Poletto P, Restelatto D, Manera C, Silva JP, Junges J, et al. Steam gasification of poultry litter biochar fo rbio-syngas production. Process Saf Environ Prot 2017;109:478–88.
[32] Farrow T, Sun C, Snape C. Impact of CO_2 on biomass pyrolysis, nitrogen partitioning, and char combustion in a drop tube furnace. J Anal Appl Pyrol 2015;113:323–31.
[33] Chen D, Cen K, Chen F, Ma Z, Zhou J, Li M. Are the typical organic components in biomass pyrolyzed bio-oil available for leaching of alkali and alkaline earth metallic species (AAEMs) from biomass? Fuel 2020;260:116347.
[34] Wang S, Dai G, Yang H, Luo Z. Lignocellulosic biomass pyrolysis mechanism: A state-of-the-art review. Prog Energy Combust Sci 2017;62:33–86.
[35] Sun Y, Bai F, Lü X, Jia C, Wang Q, Guo M, et al. Kinetic study of Huadian oil shale combustion using a multi-stage parallel reaction model. Energy 2015;82:705–13.
[36] Sobek S, Werle S. Kinetic modelling of waste wood devolatilization during pyrolysis based on thermogravimetric data and solar pyrolysis reactor performance. Fuel 2020;261:116459.
[37] Ma Q, Han L, Huang G. Evaluation of different water-washing treatments effects on

wheat straw combustion properties. Bioresour Technol 2017;245:1075–83.
[38] Demiral I, Ayan EA. Pyrolysis of grape bagasse: Effect of pyrolysis conditions on the product yields and characterization of the liquid product. Bioresour Technol 2011;102:3946–51.
[39] Hlavsová A, Corsaro A, Raclavská H, Juchelková D, Škrobánková H, Frydrych J. Syngas Production from Pyrolysis of Nine Composts Obtained from Nonhybrid and Hybrid Perennial Grasses. Hindawi Publ Corp e Sci World J 2014:1–11.
[40] Trubetskaya A, Jensen PA, Jensen AD, Steibel M, Spliethoff H, Glarborg P. Influence of fast pyrolysis conditions on yield and structural transformation of biomass chars. Fuel Process Technol 2015;140:205–14.
[41] Della Rocca PA, Cerrella EG, Bonelli PR, Cukierman AL. Pyrolysis of hardwoods residues: On kinetics and chars characterization. Biomass Bioenergy 1999;16:79–88.
[42] Kurosaki F, Ishimaru K, Hata T, Bronsveld P, Kobayashi E, Imamura Y. Microstructure of wood charcoal prepared by flash heating. Carbon 2003;41:3057–62.
[43] Fushimi C, Araki K, Yamaguchi Y, Tsutsumi A. Effect of heating rate on steam gasification of biomass. 1. Reactivity of char. Ind Eng Chem Res 2003;42:3922–8.
[44] Cetin E, Moghtaderi B, Gupta R, Wall TF. Influence of pyrolysis conditions on the structure and gasification reactivity of biomass chars. Fuel 2004;83:2139–50.
[45] Cetin E, Gupta R, Moghtaderi B. Effect of pyrolysis pressure and heating rate on radiata pine char structure and apparent gasification reactivity. Fuel 2005;84:1328–34.
[46] Guerrero M, Ruiz MP, Alzueta MU, Bilbao R, Millera A. Pyrolysis of eucalyptus at different heating rates: Studies of char characterization and oxidative reactivity. J Anal Appl Pyrol 2005;74:307–14.
[47] Hillig DM, Pohlmann JG, Manera C, Perondi D, Pereira FM, Altafini CR, et al. Evaluation of the structural changes of a char produced by slow pyrolysis of biomass and of a high-ash coal during its combustion and their role in the reactivity and flue gas emissions. Energy 2020;202:117793.
[48] Sørensen CO, Johnsson JE, Jensen A. Reduction of NO over Wheat Straw Char. Energy Fuels 2001;15:1359–68.
[49] Liu Y, Che D, Xu T. The effects of indigenous minerals in a coal on the emissions of NO and SO_2 during combustion. Combust Flame 2004;138:404–6.
[50] Bridgeman TG, Jones JM, Williams A, Waldron DJ. An investigation of the grindability of two torrefied energy crops. Fuel 2010;89:3911–8.